The Scientific Temper (2024) Vol. 15 (2): 2050-2059
E-ISSN: 2231-6396, ISSN: 0976-8653
Doi: 10.58414/SCIENTIFICTEMPER.2024.15.2.13
https://scientifictemper.com/

RESEARCH ARTICLE

Static deformation of a two-phase medium consisting of a rigid boundary elastic layer and an isotropic elastic half-space induced by a very long tensile fault

Sangeeta[1,2*], Jitander S. Sikka[2], Meenal Malik[3]

Abstract

An analytical model is proposed to determine the static response of a multi-layered medium comprising of an underlying isotropic (ISO) elastic half-space that is in welded contact with an isotropic (ISO) elastic layer of uniform thickness *H* with a rigid boundary, induced by a tensile dislocation embedded in the layer. The integral expressions for stress fields are obtained by using the airy stress function. These integrals are calculated approximately, using Sneddon's approach, by substituting the terms under the integral sign with a finite sum of exponential expressions. It is studied numerically and graphically how stresses vary with the change in the epicentral distance for different source locations embedded in the layer. The effect of the rigidity ratio is also analysed on the stress field. To examine the impact of the internal boundary, the stress fields in the layered and uniform half-spaces are compared graphically.

Keywords: Tensile fault, Welded contact, Epicentral distance, Stresses, Displacement.

Introduction

Seismology is the scientific discipline that investigates the frequency of earthquakes and the propagation of seismic waves within the Earth. Static dislocation earth models are employed to analyze the deformation fields of the medium caused by earthquake faults. The tensile fault representation model is crucial for geophysical applications such as modeling deformation fields caused by dyke injection in volcanic zones, mine collapse, and fluid-driven cracks.

Numerous researchers have extensively studied the deformation of different earth models caused by 2D sources. Inspired by the revolutionary study conducted by (Steketee, 1958a; Steketee, 1958b) on the application of the elastic theory of dislocations to analyze the deformation caused by a strike-slip fault with uniform slip in a three-dimensional model (Maruyama, 1964) derived the equations for the displacement and stress fields in a semi-infinite Poisson solid resulting from vertical and horizontal tensile faults. (Maruyama, 1966) gave detailed expressions for the Green's functions, displacement, and stress fields for a two-dimensional Poissonian media. In a multi-layered half-space, (Savage, 1998) calculated the displacement field as a Fourier integral produced by an edge dislocation. In their study, Singh and Garg (1986) examined the plane strain problem to analyze the representation of 2-D seismic sources in an unbounded medium. They derived the airy stress function and determined several source coefficients. (Rani *et al.*, 1991) considered the problem of a uniform half-space with traction-free boundary conditions at the interface due to 2-D buried sources. The integrals are analytically evaluated to derive the expressions for the airy stress function, displacement field, and stress field. In their work, (Singh and Rani, 1991) designed mathematical equations to describe the deformation field caused by two-dimensional seismic sources in a two-phase model. (Rani and Singh, 1992) studied the problem of static deformation to derive the expressions for deformation fields of a uniform half-space with a traction-free surface caused by a dip-slip fault.

[1]Department of Mathematics, IB PG College, Panipat, Haryana, India.
[2]Department of Mathematics, Maharshi Dayanand University, Rohtak, Haryana, India.
[3]Department of Mathematics, All India Jat Heroes' Memorial College, Rohtak, Haryana, India.
***Corresponding Author:** Sangeeta, Department of Mathematics, IB PG College, Panipat, Haryana, India, E-Mail: ssangeeta1529@gmail.com

How to cite this article: Sangeeta, Sikka, J. S., Malik, M. (2024). Static deformation of a two-phase medium consisting of a rigid boundary elastic layer and an isotropic elastic half-space induced by a very long tensile fault. The Scientific Temper, **15**(2):2050-2059.
Doi: 10.58414/SCIENTIFICTEMPER.2024.15.2.13
Source of support: Nil
Conflict of interest: None.

Received: 05/04/2024 **Accepted:** 10/05/2024 **Published**: 15/06/2024

Following these results, (Singh and Singh, 2000) studied the corresponding problem for a vertical tensile fault. (Singh *et al.*, 1997) studied analytically the plane strain problem of a two-phase model comprising of an overlying elastic layer with a traction-free surface and which is in welded contact with an ISO half-space caused by a very long dip-slip dislocation. Following these results, (Singh and Singh, 2004) solved the corresponding problem for tensile fault and analyzed the variation of the vertical and horizontal surface displacement for different source locations with epicentral distance from the fault. Using Sneddon's method, the integrals were calculated approximately by substituting the terms under the integral sign with a finite sum of exponential expressions. (Rani and Singh, 2007) analytically discussed the plane strain problem of two welded half-spaces caused by 2-D seismic sources. Standard integral transform tables were used to solve the expressions for the deformation fields. The drained and undrained cases for pore pressure, displacements, and stresses were also studied numerically. (Pakhare *et al.*, 2021) analytically and numerically investigate the flexure of isotropic plates using the novel first-order shear deformation theory. (Madan and Kumari, 2022) studied the plane-strain deformation for stresses and displacements for two imperfectly joined half-spaces induced by vertical tensile fault. (Chugh *et al.*, 2011) derived mathematical equations that describe the deformation of a homogeneous, orthotropic, elastic layer at any point where it interfaces with a base and this deformation is caused by a non-uniform discontinuity (slip) along a very long strike-slip fault located within the orthotropic elastic layer. Four non-uniform slip profiles, namely linear, parabolic, and cubic, are taken into account when considering the fault. Using the eigenvalue approach, (Madan and Gaba, 2016) calculated the displacement and stresses at every location in an infinite irregular orthotropic elastic material induced by a normal line load. They have considered the irregularities of parabolic and rectangular. (Manna and Sen, 2017) examined two inclined, interacting, strike-slip, faults that are buried under a viscoelastic layer. These faults are located on and in welded contact with a viscoelastic half-space, which represents the lithosphere-asthenosphere system. (Kundu *et al.*, 2021) considered an analytical study for displacement, stress, and strain due to creeping, buried, finite strike-slip fault inclined to the vertical at an arbitrary angle. The fault is situated in an elastic layer over an elastic half-space representing the lithosphere-asthenosphere system. (Kundu and Sarkar, 2021) studied the deformation of an elastic layer that is on top of an elastic half-space. This deformation is induced by a finite, buried, inclined, locked strike-slip fault. (Kumari and Madan, 2022) incorporated into their mathematical model the stresses induced by vertical dip-slip faults that are embedded in an isotropic half-space perfectly joined with an orthotropic half-space. (Savita *et al.*, 2022) proposed an analytical model to describe the static deformation of a two-dimensional system. This system consists of a layer of uniform thickness made of a homogeneous isotropic elastic material put on top of an irregular isotropic elastic half-space. The deformation is caused by the movement of a long tensile fault. (Soni and Rani, 2023) obtained a detailed solution for the plane strain deformation of a two-layer model consisting of a homogeneous, elastically isotropic substratum indued by two-dimensional faulting located in the isotropic stratum. (Sangeeta *et al.*, 2023) derived static deformation caused by a tensile fault embedded in an isotropic half-space perfectly joined with an orthotropic half-space. Using the fourier transform method, (Rani and Rani, 2024) examined the antiplane deformation of a two-layered elastic medium model induced by an inclined long strike-slip fault

Our main aim of the paper is to mathematically analyze the plane strain problem for a multi-layered model. This multi-layered model consists of a rigid boundary layer of thickness *H* lying over an ISO half-space caused by a tensile dislocation embedded in the overlying layer. The overlying layer is assumed to be with rigid boundary along z = 0 and the interface of both the media along the plane z = H are to be taken in welded contact. The procedure employed by (Singh *et al.*, 1997) is used to obtain the stress field due to horizontal tensile fault and vertical tensile fault. This procedure makes use of various forward Laplace transforms and then inverse Laplace transforms. The stresses caused by both horizontal tensile fault and vertical tensile are numerically evaluated for three different source depths. The stress fields for layered and uniform half-spaces are compared numerically as well as graphically.

Materials and Methods

Let the cartesian coordinate system be denoted by $(x_1, x_2, x_3) \equiv (x, y, z)$ with the z-axis vertically downwards. We examine a multi-layered model comprising of an ISO elastic layer of uniform thickness H lying over an ISO elastic half-space, which are to be taken in welded contact along the plane $z = H$. A 2-D approximation is considered in which the displacement components (u_1, u_2, u_3) are independent of x so that $\partial/\partial x \equiv 0$. In this paper, the sources considered are infinitely thin strips with opposite Burgers vectors and both are placed at an infinitesimal distance ds.

For a line dislocation, the airy stress function U_0, given by (Singh and Garg, 1986) as:

$$U_0 = \int_0^\infty [(L_0 + M_0 k|z-h|)\ sin\ ky + (P_0 + Q_0 k|z-h|)\ cos\ ky] k^{-1} e^{-k|z-h|}\ dk \quad (1)$$

where, L_0, M_0, P_0, Q_0 (source coefficients) are independent of k.

The overlying layer is considered to be medium I and the underlying half-space is considered to be medium II. For a

line dislocation passing through the point $(0,0,h)$ of the overlying layer (medium I), the airy stress function is given by (Singh and Garg, 1986; Rani and Singh, 2007; Sangeeta *et al.*, 2023)

$$U^{(1)} = U_0 + \int_0^\infty [(L_1 + M_1 kz)\ sin\ ky + (P_1 + Q_1 kz)\ cos\ ky]k^{-1}e^{-kz}\ dk + \int_0^\infty [(L_2 + M_2 kz)\ sin\ ky + (P_2 + Q_2 kz)\ cos\ ky]k^{-1}e^{-kz}\ dk \quad (2)$$

and the airy stress function for medium II may be of the form

$$U^{(2)}\ \int_0^\infty [(L_3 + M_3 kz)\ sin\ ky + (P_3 + Q_3 kz)\ cos\ ky]k^{-1}e^{-kz}\ dk \quad (3)$$

where the airy stress function U_0 is given by Eq. (1) and using the boundary conditions, the unknowns L_1, M_1, etc. are to be determined in terms of the source coefficients.

The expressions for stresses and displacements, using the airy stress function, are given by (Sokolnikoff and Specht, 1956)

$$\tau_{22}^{(r)} = \frac{\partial^2 U^{(r)}}{\partial z^2}, \tau_{33}^{(r)} = \frac{\partial^2 U^{(r)}}{\partial y^2}, \tau_{23}^{(r)} = -\frac{\partial^2 U^{(r)}}{\partial y \partial z} \quad (4)$$

$$2\mu_r u_2^r = -\frac{\partial U^{(r)}}{\partial y} + \frac{1}{2\alpha_r}\int \nabla^2 U^{(r)} dy \quad (5)$$

$$2\mu_r u_3^r = -\frac{\partial U^{(r)}}{\partial z} + \frac{1}{2\alpha_r}\int \nabla^2 U^{(r)} dz \quad (6)$$

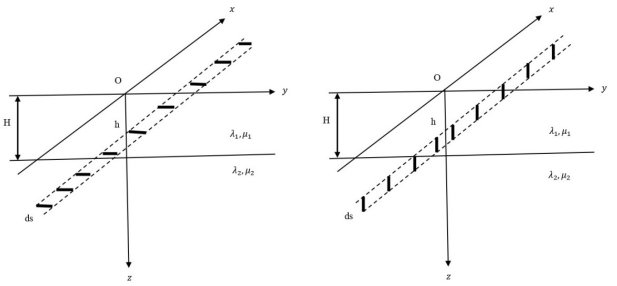

(a) (b)

Figure 1: Illustrates the geometric characteristics of a line dislocation with finite widths ds and infinite length and the dislocation is embedded in a layer situated above a half-space at the point (0,0,h).

where $\alpha_r = \frac{\lambda_r + \mu_r}{\lambda_r + 2\mu_r} = \frac{1}{2(1-\sigma_r)}$ (7)

$$\Delta^2 U^{(r)} = \tau_{22}^{(r)} + \tau_{33}^{(r)} \quad (8)$$

σ denotes the Poisson's ratio. In Eqs. (4)-(8), $r = 1$ and $r = 2$ are used for medium I and medium II, respectively. The Figure 1 represents two types of faults: (a) a horizontal tensile fault and (b) a vertical tensile fault (Singh and Singh, 2004)

Using Eqs. (1)-(3) in Eqs. (4)-(8), for medium I and medium II, the expressions for stresses and displacements are given by

$$\tau_{22}^{(1)} = \int_0^\infty \left[(L_0 - 2M_0 + M_0 k|z-h|)e^{-k|z-h|} + (L_1 - 2M_1 + M_1 kz)e^{-kz} + (L_2 + 2M_2 + M_2 kz)e^{kz}\right] k \sin ky\ dk + \int_0^\infty \left[(P_0 - 2Q_0 + Q_0 k|z-h|)e^{-k|z-h|} + (P_1 - 2Q_1 + Q_1 kz)e^{-kz} + (P_2 + 2Q_2 + Q_2 kz)e^{kz}\right] k \cos ky\ dk \quad (9)$$

$$\tau_{23}^{(1)} = \int_0^\infty \left[\pm(L_0 + M_0 + M_0 k|z-h|)e^{-k|z-h|} + (L_1 - M_1 + M_1 kz)e^{-kz} - (L_2 + M_2 + M_2 kz)e^{kz}\right] k \cos ky\ dk - \int_0^\infty \left[\pm(P_0 + Q_0 + Q_0 k|z-h|)e^{-k|z-h|} + (P_1 - Q_1 + Q_1 kz)e^{-kz} - (P_2 + Q_2 + Q_2 kz)e^{kz}\right] k \sin ky\ dk \quad (10)$$

$$\tau_{33}^{(1)} = \int_0^\infty \left[(L_0 + M_0 k|z-h|)e^{-k|z-h|} + (L_1 + M_1 kz)e^{-kz} + (L_2 + M_2 kz)e^{kz}\right] k \sin ky\ dk - \int_0^\infty \left[(P_0 + Q_0 k|z-h|)e^{-k|z-h|} + (P_1 + Q_1 kz)e^{-kz} + (P_2 + Q_2 kz)e^{kz}\right] k \cos ky\ dk \quad (11)$$

$$\tau_{22}^{(2)} = \int_0^\infty [(L_3 - 2M_3 + M_3 kz)\sin ky + (P_3 - 2Q_3 + Q_3 kz)\cos ky]\ k\ e^{-kz}\ dk \quad (12)$$

$$\tau_{23}^{(2)} = \int_0^\infty [(L_3 - M_3 + M_3 kz)\cos ky - (P_3 - Q_3 + Q_3 kz)\sin ky]\ k\ e^{-kz}\ dk \quad (13)$$

$$\tau_{33}^{(2)} = -\int_0^\infty [(L_3 + M_3 kz)\sin ky + (P_3 + Q_3 kz)\cos ky]\ k\ e^{-kz}\ dk \quad (14)$$

$$2\mu_1\mu_2^{(1)} = -\int_0^\infty \left[\left(L_0 + M_0 k|z-h| - \tfrac{1}{\alpha_1}M_0\right)e^{-k|z-h|} + \left(L_1 + M_1 kz - \tfrac{1}{\alpha_1}M_1\right)e^{-kz} + \left(L_2 + M_2 kz + \tfrac{1}{\alpha_1}M_2\right)e^{kz}\right]\cos ky\ dk + \int_0^\infty \left[\left(P_0 + Q_0 k|z-h| - \tfrac{1}{\alpha_1}Q_0\right)e^{-k|z-h|} + \left(P_1 + Q_1 kz - \tfrac{1}{\alpha_1}Q_1\right)e^{-kz} + \left(P_2 + Q_2 kz + \tfrac{1}{\alpha_1}Q_2\right)e^{kz}\right]\sin ky\ dk \quad (15)$$

$$2\mu_1\mu_3^{(1)} = \int_0^\infty \left[\pm\left(L_0 - M_0 + M_0 k|z-h| + \tfrac{1}{\alpha_1}M_0\right)e^{-k|z-h|} + \left(L_1 - M_1 + M_1 kz + \tfrac{1}{\alpha_1}M_1\right)e^{-kz} - \left(L_2 + M_2 + M_2 kz - \tfrac{1}{\alpha_1}M_2\right)e^{kz}\right]\sin ky\ dk + \int_0^\infty \left[\pm\left(P_0 - Q_0 + Q_0 k|z-h| + \tfrac{1}{\alpha_1}Q_0\right)e^{-k|z-h|} + \left(P_1 - Q_1 + Q_1 kz + \tfrac{1}{\alpha_1}Q_1\right)e^{-kz} - \left(P_2 - Q_2 + Q_2 kz - \tfrac{1}{\alpha_1}Q_2\right)e^{kz}\right]\cos ky\ dk \quad (16)$$

$$2\mu_2\mu_2^{(2)} = \int_0^\infty \left[-\left(L_3 + M_3 kz - \frac{1}{\alpha_2}M_3\right)\cos ky + \left(P_3 + Q_3 kz - \frac{1}{\alpha_2}Q_3\right)\sin ky\right] e^{-kz}\, dk \tag{17}$$

$$2\mu_2\mu_3^{(2)} = \int_0^\infty \left[\left(L_3 - M_3 + M_3 kz + \frac{1}{\alpha_2}M_3\right)\sin ky + \left(P_3 - Q_3 + Q_3 kz + \frac{1}{\alpha_2}Q_3\right)\cos ky\right] e^{-kz}\, dk \tag{18}$$

Since, we have assumed that the overlying layer $(z = 0)$ is with rigid boundary and the half-space and layer are to be taken in welded contact along the plane $z = H$. Therefore, the boundary conditions are

$$\begin{aligned} &u_2^{(1)} = u_3^{(1)} = 0 \text{ at } z = 0 \\ &\tau_{23}^{(1)} = \tau_{23}^{(2)}, \tau_{33}^{(1)} = \tau_{33}^{(2)} \text{ at } z = H \\ &u_2^{(1)} = u_2^{(2)}, u_3^{(1)} = u_3^{(2)} \text{ at } z = H \end{aligned} \tag{19}$$

Let $L^{\pm}, M^{\pm}, P^{\pm}, Q^{\pm}$ be the values of source coefficients L_0, M_0, P_0, Q_0 valid for $z \geq h$. Then, using Eq. (10) and Eq. (11) and Eqs. (13)-(18) in Eq. (11), we get two sets of system of equations, one is in $L_1, M_1, L_2, M_2, L_3, M_3$ and the other is in $P_1, Q_1, P_2, Q_2, P_3, Q_3$ and these systems of equations in matrix form can be written as

$$J\begin{bmatrix} L_1 \\ L_2 \\ L_3 \\ M_1 \\ M_2 \\ M_3 \end{bmatrix} = \begin{bmatrix} -(L^- + M^- kh - M^-/\alpha_1)e^{-kh} \\ (L^- - M^- + M^- kh + M^-/\alpha_1)e^{-kh} \\ -(L^+ - M^+ + M^+ k(H-h))e^{-k(H-h)} \\ -(L^+ + M^+ k(H-h))e^{-k(H-h)} \\ (L^+ + M^+ k(H-h) - M^+/\alpha_1)e^{-k(H-h)} \\ -(L^+ - M^+ + M^+ k(H-h) + M^+/\alpha_1)e^{-k(H-h)} \end{bmatrix} \tag{20}$$

and

$$J\begin{bmatrix} P_1 \\ P_2 \\ P_3 \\ Q_1 \\ Q_2 \\ Q_3 \end{bmatrix} = \begin{bmatrix} -(P^- + Q^- kh - Q^-/\alpha_1)e^{-kh} \\ (P^- - Q^- + Q^- kh + Q^-/\alpha_1)e^{-kh} \\ -(P^+ - Q^+ + Q^+ k(H-h))e^{-k(H-h)} \\ -(P^+ + Q^+ k(H-h))e^{-k(H-h)} \\ (P^+ + Q^+ k(H-h) - Q^+/\alpha_1)e^{-k(H-h)} \\ -(P^+ - Q^+ + Q^+ k(H-h) + Q^+/\alpha_1)e^{-k(H-h)} \end{bmatrix} \tag{21}$$

Where J is the 6×6 matrix given by

$$J = \begin{bmatrix} 1 & 1 & 0 & -\frac{1}{\alpha_1} & \frac{1}{\alpha_1} & 0 \\ 1 & -1 & 0 & \left(\frac{1}{\alpha_1} - 1\right) & \left(\frac{1}{\alpha_1} - 1\right) & 0 \\ e^{-kH} & -e^{kH} & -e^{-kH} & (kH-1)e^{-kH} & -(kH+1)e^{kH} & (1-kH)e^{-kH} \\ e^{-kH} & e^{kH} & -e^{-kH} & kHe^{-kH} & kHe^{kH} & -kHe^{-kH} \\ -e^{-kH} & -e^{kH} & \beta e^{-kH} & \left(\frac{1}{\alpha_1} - kH\right)e^{-kH} & -\left(\frac{1}{\alpha_1} + kH\right)e^{kH} & \beta\left(kH - \frac{1}{\alpha_2}\right)e^{-kH} \\ e^{-kH} & -e^{kH} & -\beta e^{-kH} & \left(\frac{1}{\alpha_1} - 1 + kH\right)e^{-kH} & -\left(1 + kH - \frac{1}{\alpha_1}\right)e^{kH} & -\beta\left(\frac{1}{\alpha_2} - 1 + kH\right)e^{-kH} \end{bmatrix}$$

Now using Cramer's rule, solving the system of Eqs. (20) and (21), we obtain

$$\begin{aligned} L_1 = &\frac{1}{4\delta^2 v^2 \delta_1 \Delta}\Big[\Big\{Z_1(1 + 2Hk\delta^2)(L^+ - M^+ kh) + Z_1 Hk\delta^2(-1 + 2Hk)M^+ + \\ &\frac{1}{2}(Z_1 + Z_4)M^+\Big\}e^{-k(2H-h)} + \Big\{\delta Z_1(-1 + 2Hk)(L^- + M^- kh) - 2H^2k^2\delta Z_1 M^- + \frac{1}{2\delta}(\delta^2 Z_1 - \\ &Z_4)M^-\Big\}e^{-k(2H+h)} + Z_3\Big\{\delta(L^- + M^- kh) + \frac{1}{2\delta}(1-\delta)M^-\Big\}e^{-kh} + Z_2(L^+ - M^+ kh)e^{-k(4H-h)}\Big] \end{aligned} \tag{22}$$

$$\begin{aligned} L_2 = &\frac{1}{4\delta^2 v^2 \delta_1 \Delta}\Big[\Big\{\delta Z_1(1 + 2Hk)(L^+ - M^+ kh) + 2H^2k^2\delta Z_1 M^+ + \frac{1}{2\delta}(-\delta^2 Z_1 + Z_4)M^+\Big\}e^{-k(2H-h)} + \\ &\Big\{\Big(\frac{Z_4}{2} + Z_1 Hk\delta^2(1 + 2Hk)\Big)(L^- + (-1 + 2hk)M^-) + \frac{Z_4}{2}(1 + 2Hk)M^-\Big\}e^{-k(2H+k)} - \\ &Z_2\{(L^- + M^- kh)\}e^{-k(4H+h)} - Z_2\Big\{\delta(L^+ - M^+ kh) + \frac{(1-\delta^2)M^+}{2\delta}\Big\}e^{-k(4H-h)}\Big] \end{aligned} \tag{23}$$

$$L_3 = \frac{(1+\delta)}{2\delta^2 v\,\delta_1\Delta}\Big[\Big\{2(1+\delta_1 v)L^+ + (-1-2hk+2Hk)(1+\delta_1 v)M^+ + \frac{\delta_1(v+\delta)(1-2Hk)}{\delta}M^+\Big\}e^{kh} + \Big\{2Hk\delta(2L^- + (1-2Hk)M^-) + \frac{(1+v\delta_1)}{\delta}M^- + \delta_1\big(\delta + 2Hk\delta(-1+v) + v(1-2Hk)\big)(2L^- + (-1+2hk)M^-)\Big\}e^{-kh} + \Big\{\delta_1(-1+v)(-1+2Hk)(2L^- + (-1+2hk-2Hk)M^-) + \frac{(\delta+v\delta_1)}{\delta}M^-\Big\}e^{-k(2H+h)} - \Big\{(v\delta_1-\delta)L^+ + (\delta+v\delta_1)(1+2hk)M^+ - \frac{\delta_1}{\delta}(-1+2Hk)(-1+v)M^+ + 2Hk\delta\delta_1(-1+2Hk)\times\big((-1+v)L^+ + v\delta_1(1+2hk)M^+\big) + v\delta_1(1+2hk)M^+\Big\}e^{-k(2H-h)}\Big] \quad (24)$$

$$M_1 = \frac{1}{4\delta^2 v^2\,\delta_1\Delta}\big[\delta Z_3\{2L^- + (-1+2hk)M^-\}e^{-kh} - Z_2 M^+ e^{-k(4H-h)} + \{4Hk\delta^2 Z_1 L^+ + (2Hk\,\delta^2 Z_1(-1-2hk+2Hk) + Z_4)M^+\}e^{-k(2H-h)} - \delta Z_1\{2L^- + (-1+2hk-2Hk)M^-\}e^{-k(2H+h)}\big] \quad (25)$$

$$M_2 = \frac{1}{4\delta^2 v^2\,\delta_1\Delta}\big[\delta Z_2\{2L^+ - (1+2hk)M^+\}e^{-k(4H-h)} + \delta Z_2 M^- e^{-k(4H+h)} - Z_1\{4Hk\delta^2(L^- + M^- kh) + (1-2Hk\delta^2)M^-\}e^{-k(2H+h)} - \delta Z_1\{2L^+ + (-1-2hk+2Hk)M^+\}e^{-k(2H-h)}\big] \quad (26)$$

$$M_3 = \frac{1+\delta}{\delta^2 v\,\Delta}\Big[(v+\delta)\{2L^- + (-1+2hk)M^-\}e^{-kh} + \frac{(v+\delta)}{v}M^+ e^{kh} + (1-v)\{2L^- + (-1+2hk-2Hk)M^-\}e^{-k(2H+h)} + (1-v)\Big\{4Hk\delta(-L^+ + M^+ kh) + \frac{(1+2Hk\,\delta^2)}{\delta}M^+\Big\}e^{-k(2H-h)}\Big] \quad (27)$$

$$P_1 = \frac{1}{4\delta^2 v^2\,\delta_1\Delta}\Big[\Big\{Z_1(1+2Hk\delta^2)(P^+ - Q^+ kh) + Z_1 Hk\delta^2(-1+2Hk)Q^+ + \frac{1}{2}(Z_1+Z_4)Q^+\Big\}e^{-k(2H-h)} + \Big\{\delta Z_1(-1+2Hk)(P^- + Q^- kh) - 2H^2k^2\delta Z_1 Q^- + \frac{1}{2\delta}(\delta^2 Z_1 - Z_4)Q^-\Big\}e^{-k(2H+h)} + Z_3\Big\{\delta(P^- + Q^- kh) + \frac{1}{2\delta}(1-\delta)Q^-\Big\}e^{-kh} + Z_2(P^+ - Q^+ kh)e^{-k(4H-h)}\Big] \quad (28)$$

$$P_2 = \frac{1}{4\delta^2 v^2\,\delta_1\Delta}\Big[\Big\{\delta Z_1(1+2Hk)(P^+ - Q^+ kh) + 2H^2k^2\delta Z_1 Q^+ + \frac{1}{2\delta}(-\delta^2 Z_1 + Z_4)Q^+\Big\}e^{-k(2H-h)} + \Big\{\Big(\frac{Z_4}{2} + Z_1 Hk\delta^2(1+2Hk)\Big)(P^- + (-1+2hk)Q^-) + \frac{Z_4}{2}(1+2Hk)Q^-\Big\}e^{-k(2H+h)} - Z_2\{(P^- + Q^- kh)\}e^{-k(4H+h)} - Z_2\Big\{\delta(P^+ - Q^+ kh) + \frac{(1-\delta^2)Q^+}{2\delta}\Big\}e^{-k(4H-h)}\Big] \quad (29)$$

$$P_3 = \frac{(1+\delta)}{2\delta^2 v\,\delta_1\Delta}\Big[\Big\{2(1+\delta_1 v)P^+ + (-1-2hk+2Hk)(1+\delta_1 v)Q^+ + \frac{\delta_1(v+\delta)(1-2Hk)}{\delta}Q^+\Big\}e^{kh} + \Big\{2Hk\delta(2P^- + (1-2Hk)Q^-) + \frac{(1+v\delta_1)}{\delta}Q^- + \delta_1(\delta + 2Hk\delta(-1+v) + v(1-2Hk))(2P^- + (-1+2hk)Q^-)\Big\}e^{-kh} + \Big\{\delta_1(-1+v)(-1+2Hk)(2P^- + (-1+2hk-2Hk)Q^-) + \frac{(\delta-v\delta_1)}{\delta}Q^-\Big\}e^{-k(2H+h)} - \Big\{(v\delta_1-\delta)P^+ + (\delta+v\,\delta_1)(1+2hk)Q^+ - \frac{\delta_1}{\delta}(-1+2Hk)(-1+v)Q^+ + 2Hk\delta\delta_1(-1+2Hk)\times\big((-1+v)P^+ + v\delta_1(1+2hk)Q^+\big) + v\delta_1(1+2hk)Q^+\Big\}e^{-k(2H-h)}\Big] \quad (30)$$

$$Q_1 = \frac{1}{4\delta^2 v^2\,\delta_1\Delta}\big[\delta Z_3\{2P^- + (-1+2hk)Q^-\}e^{-kh} - Z_2 Q^+ e^{-k(4H-h)} + \{4Hk\delta^2 Z_1 P^+ + (2Hk\delta^2 Z_1(-1-2hk+2Hk) + Z_4)Q^+\}e^{-k(2H-h)} - \delta Z_1\{2P^- + (-1+2hk-2Hk)Q^-\}e^{-k(2H+h)}\big] \quad (31)$$

$$Q_2 = \frac{1}{4\delta^2 v^2\,\delta_1\Delta}\big[\delta Z_2\{2P^+ - (1+2hk)Q^+\}e^{-k(4H-h)} + \delta Z_2 Q^- e^{-k(4H+h)} - Z_1\{4Hk\delta^2(P^- + Q^- kh) + (1-2Hk\delta^2)Q^-\}e^{-k(2H+h)} - \delta Z_1\{2P^+ + (-1-2hk+2Hk)Q^+\}e^{-k(2H-h)}\big] \quad (32)$$

$$Q_3 = \frac{1+\delta}{\delta^2 v\,\Delta}\Big[(v+\delta)\{2P^- + (-1+2hk)Q^-\}e^{-kh} + (1-v)\{2P^- + (-1+2hk-2Hk)Q^-\}e^{-k(2H+h)} + \frac{v+\delta}{v}Q^+ e^{kh} + (1-v)\Big\{4Hk\delta(-P^+ + Q^+ kh) + \frac{(1+2Hk\,\delta^2)}{\delta}Q^+\Big\}e^{-k(2H-h)}\Big] \quad (33)$$

where $\Delta = -\frac{1}{4\delta^2 v^2\,\delta_1}[-Z_3 + (Z_1 + Z_4 + 4\delta^2 Z_1 H^2 k^2)e^{-2Hk} - Z_2 e^{-4Hk}]$ (34)

$$Z_1 = 4(v-1)(v\delta_1+1), Z_2 = 4(v-1)(v\delta_1-\delta), Z_3 = 4(v+\delta)(v\delta_1+1), Z_4 = 4(v+\delta)(v\delta_1-\delta),$$

$$\frac{1}{\delta} = \frac{2}{\alpha_1} - 1 = 3 - 4\sigma_1, \frac{1}{\delta_1} = \frac{2}{\alpha_2} - 1 = 3 - 4\sigma_2, \frac{\mu_2}{\mu_1} = \frac{1}{\beta} = v \quad (35)$$

The values defined for Z_1, Z_2, Z_3, Z_4 in Eq. (35) are given by (Ben-Menahem and Singh, 1986).

On putting $z = 0$ and then the values of the unknowns L_1, M_1 etc. From Eqs. (22)-(33) into Eq. (10) and Eq. (11), the expressions for stresses in the overlying layer are given by

$$\tau_{23}^{(1)} = \int_0^\infty \Big[\Big\{\frac{1}{4\delta^2 v^2 \delta_1 \alpha_1 \Delta}\big[\delta Z_3\{-2L^- + (1-2hk)M^-\}e^{-kh} + Z_2\{2\delta(-L^+ + M^+kh) + (1+\delta)M^+\}e^{-k(4H-h)} - Z_2 M^- e^{-k(4H+h)} + Z_1\{2\delta(1+2Hk\delta)(L^- + M^-kh) + M^- - \delta(1+2Hk(1+\delta)+1)M^-\}e^{-k(2H+h)} - \{2\delta Z_1(-1+2Hk\delta)L^+ + (\delta Z_1 + Z_4)M^+ + 2\delta Z_1 k(-h+2Hk\delta(h-H)+(1+\delta)H)M^+\}e^{-k(2H-h)}\big] + \frac{M^-}{\alpha_1}e^{-kh}\Big\}\, k\cos ky - \Big\{\frac{1}{4\delta^2 v^2 \delta_1 \alpha_1 \Delta}\big[\delta Z_3\{-2P^- + (1-2hk)Q^-\}e^{-kh} + Z_2\{2\delta(-P^+ + Q^+kh) + (1+\delta)Q^+\}e^{-k(4H-h)} - Z_2 Q^- e^{-k(4H+h)} + Z_1\{2\delta(1+2Hk\delta)(P^- + Q^-kh) + (Q^- - \delta(1+2Hk(1+\delta)+1)Q^-\}e^{-k(2H+h)} - \{2\delta Z_1(-1+2Hk\delta)P^+ + (\delta Z_1 + Z_4)Q^+ + 2\delta Z_1 k(-h+2Hk\delta(h-H)+(1+\delta)H)Q^+\}e^{-k(2H-h)}\big] + \frac{Q^-}{\alpha_1}e^{-kh}\Big\}\, k\sin ky\Big]\, dk \tag{36}$$

$$\tau_{33}^{(1)} = \int_0^\infty \Big[\Big\{\frac{1}{4\delta^2 v^2 \delta_1 \alpha_1 \Delta}\big[-\delta Z_3\{2L^- + (-1+2hk)M^-\}e^{-kh} - Z_2\{2\delta(-L^+ + M^+kh) + (\delta-1)M^+\}e^{-k(4H-h)} + Z_2 M^- e^{-k(4H+h)} - Z_1\{2\delta(2Hk\delta-1)(L^- + M^-kh) + M^- + \delta\big(1+2Hk(1-\delta)\big)M^-\}e^{-k(2H+h)} - \{2\delta Z_1(1+2Hk\delta)L^+ + (-\delta Z_1 + Z_4)M^+ + 2\delta Z_1 k(h+2Hk\delta(h-H)+(-1+\delta)H)M^+\}e^{-k(2H-h)}\big] - \frac{M^-}{\alpha_1}e^{-kh}\Big\}\, k\sin ky - \Big\{\frac{1}{4\delta^2 v^2 \delta_1 \alpha_1 \Delta}\big[-\delta Z_3\{2P^- + (-1+2hk)Q^-\}e^{-kh} - Z_2\{2\delta(-P^+ + Q^+kh) + (\delta-1)Q^+\}e^{-k(4H-h)} + Z_2 Q^- e^{-k(4H+h)} - Z_1\{2\delta(2Hk\delta-1)(P^- + Q^-kh) + Q^- + \delta\big(1+2Hk(1-\delta)\big)Q^-\}e^{-k(2H+h)} - \{2\delta Z_1(1+2Hk\delta)P^+ + (-\delta Z_1 + Z_4)Q^+ + 2\delta Z_1 k(h+2Hk\delta(h-H)+(-1+\delta)H)Q^+\}e^{-k(2H-h)}\big] - \frac{Q^-}{\alpha_1}e^{-kh}\Big\}\, k\cos ky\Big]\, dk \tag{37}$$

Tensile Fault

Two tensile dislocations are considered, one is a horizontal tensile fault and the other is a vertical tensile fault with dislocations in the z-direction and y-direction respectively.

Horizontal tensile fault

The source coefficients are given by (Singh and Rani, 1991)

$L^- = M^- = L^+ = M^+ = 0, P^- = Q^- = P^+ = Q^+ = \frac{\alpha_1 \mu_1 b ds}{\pi}$, where b is the magnitude of the displacement discontinuity and ds is the infinitesimal distance between two line dislocations.

On putting the values of the source coefficients in the expressions for stress field for the overlying layer, we obtain

$$\tau_{23}^{(1)} = \frac{\mu b ds}{\pi}\int_0^\infty \Big[\frac{1}{4\delta^2 v^2 \delta_1 \Delta}\big\{Z_2 e^{-k(4H+h)} - Z_2[1+\delta(-1+2hk)]e^{-k(4H-h)} + \big[Z_4 - \delta Z_1 - 2\delta Z_1 k\big(H-h+H\delta(-1-2Hk+2hk)\big)\big]e^{-k(2H-h)} - Z_1[2Hk\delta^2(1+2hk) + \delta(1+2hk-2Hk)+1]e^{-k(2H+h)} + \delta Z_3(1+2hk)e^{-kh}\big\} - e^{-kh}\Big]\, k\sin ky\, dk \tag{38}$$

$$\tau_{33}^{(1)} = \frac{\mu_1 b ds}{\pi}\int_0^\infty \Big[\frac{1}{4\delta^2 v^2 \delta_1 \Delta}\big\{Z_2 e^{-k(4H+h)} + Z_2[1-\delta(-1+2hk)]e^{-k(4H-h)} - \big[Z_4 + \delta Z_1 - 2\delta Z_1 k\big(-H+h+H\delta(-1-2Hk+2hk)\big)\big]e^{-k(2H-h)} - Z_1[2Hk\delta^2(1+2hk) + \delta(-1-2hk+2Hk)+1]e^{-k(2H+h)} - \delta Z_3(1+2hk)e^{-kh}\big\} - e^{-kh}\Big]\, k\cos ky\, dk \tag{39}$$

Vertical tensile fault

The source coefficients are given by (Singh and Rani, 1991)

$L^- = L^+ = M^- = M^+ = 0, P^- = P^+ = \frac{\mu_1 \alpha_1 b ds}{\pi}, Q^- = Q^+ = -\frac{\mu_1 \alpha_1 b ds}{\pi}$

On putting the values of source coefficients in the expressions for stress field for the overlying layer, we obtain

$$\tau_{23}^{(1)} = \frac{\mu_1 b ds}{\pi}\int_0^\infty \Big[\frac{1}{4\delta^2 v^2 \delta_1 \Delta}\big\{-Z_2 e^{-k(4H+h)} + Z_2[1+\delta(3+2hk)]e^{-k(4H-h)} + \big[-Z_4 - 3\delta Z_1 k\big(H-h+H\delta(3-2Hk+2hk)\big)\big]e^{-k(2H-h)} + Z_1[2Hk\delta^2(-3+2hk) + \delta(-3+2hk-2Hk)+1]e^{-k(2H+h)} + \delta Z_3(3-2hk)e^{-kh}\big\} + e^{-kh}\Big]\, k\sin ky\, dk \tag{40}$$

$$\tau_{33}^{(1)} = \frac{\mu_1 b ds}{\pi}\int_0^\infty \Big[\frac{1}{4\delta^2 v^2 \delta_1 \Delta}\big\{-Z_2 e^{-k(4H+h)} + Z_2[-1+\delta(3+2hk)]e^{-k(4H-h)} - \big[-Z_4 + 3\delta Z_1 + 2\delta Z_1 k\big(-H+h+H\delta(3-2Hk+2hk)\big)\big]e^{-k(2H-h)} + Z_1[2Hk\delta^2(-3+2hk) + \delta(3-2hk+2Hk)+1]e^{-k(2H+h)} + \delta Z_3(-3+2hk)e^{-kh}\big\} + e^{-kh}\Big]\, k\cos ky\, dk \tag{41}$$

Uniform Half-Space

For a uniform half-space, the expressions of the stress field can be obtained by taking the limit $H \to \infty$ in the expressions of the stress field of the layer overlying a uniform half-space. Consequently, for a horizontal tensile fault, the expressions for the stress field are given by

$$\tau_{23} = \frac{\mu_1 b ds}{\pi} \int_0^\infty hk^2 e^{-kh} \sin ky \, dk \tag{42}$$

$$\tau_{33} = -\frac{\mu_1 b ds}{\pi} \int_0^\infty k(1+hk) e^{-kh} \cos ky \, dk \tag{43}$$

Integrating Eq. (42) and Eq. (43), we obtain

$$\tau_{23} = \frac{\mu_1 b ds}{\pi} \left[-\frac{2hy\,(-3h^2+y^2)}{(h^2+y^2)^2} \right] \tag{44}$$

$$\tau_{33} = \frac{\mu_1 b ds}{\pi} \left[\frac{-3h^4+6h^2y^2+y^4}{(h^2+y^2)^2} \right] \tag{45}$$

Similarly, for a vertical tensile fault, from Eq. (40) and Eq. (41) we obtain

$$\tau_{23} = \frac{\mu_1 b ds}{\pi} \int_0^\infty k(2-hk) e^{-kh} \sin ky \, dk \tag{46}$$

$$\tau_{33} = -\frac{\mu_1 b ds}{\pi} \int_0^\infty k(1-hk) e^{-kh} \cos ky \, dk \tag{47}$$

Integrating Eq. (46) and Eq. (47), we obtain

$$\tau_{23} = \frac{\mu_1 b ds}{\pi} \left[-\frac{2hy(h^2-3y^2)}{(h^2+y^2)^2} \right] \tag{48}$$

$$\tau_{33} = \frac{\mu_1 b ds}{\pi} \left[\frac{h^4-6h^2y^2+y^4}{(h^2+y^2)^2} \right] \tag{49}$$

Results

The integral expressions appearing in Eqs. (38)-(41) can be written in the form

$$\int_0^\infty \frac{G}{\Delta} e^{-kp} k^q \begin{pmatrix} \cos ky \\ \sin ky \end{pmatrix} dk \tag{50}$$

where, $G = \frac{Z_3}{4\delta^2 v^2 \delta_1}, q = 1, 2, 3;$

$$p = h, 2H \pm h, 4H \pm h \tag{51}$$

The factor $\frac{1}{\Delta}$ involved in the integrand of the above integrals renders integration by analytical methods difficult. However, (Sneddon, 1951) advised an approximation by which this difficulty is overcome and the idea was that the factor $\frac{1}{\Delta}$ can be substituted by a sum of exponential terms in order to make the error as small as we looked for.

From Eq. (34) and Eq. (51), we have

$$\frac{G}{\Delta} = \frac{1}{1-((A+Bk^2H^2)e^{-2Hk}-De^{-4Hk})} \tag{52}$$

where, $A = \frac{Z_1+Z_4}{Z_3}, B = \frac{4\delta^2 Z_1}{Z_3}, D = \frac{Z_2}{Z_3}$

Applying binomial expansion in Eq. (52), we have

$$\frac{G}{\Delta} = 1 + (A+Bk^2H^2)e^{-2kH} + (A^2 - D + B^2k^4H^4 + 2ABk^2H^2)e^{-2kH} + \cdots \tag{53}$$

Following, (Ben-Menahem and Gillon, 1970), we take approximation

$$\frac{G}{\Delta} \cong 1 + (A+Bk^2H^2)e^{-nkH} + (C+\alpha' k^n H^n)e^{-\beta' kH} \tag{54}$$

where, $C = \frac{A^2-D(A+1)}{1-A+D}, n = 1, 2, 3, 4, \ldots$ (55)

and α', $\beta' (> 2)$ areto be taken in such a manner so as to make a best fit in the least-square sense. Putting $H = 0$, in Eq. (52) and Eq. (54) and equating both equations we obtained the value of C. By the usage of approximation (54), a linear combination of known integrals, of the form (Gradshteyn *et al.*, 1988) is used to approximate the integrals appearing in Eq. (50).

$$C_m(x,y) = \int_0^\infty k^m e^{-kx} \cos ky \, dk = (-1)^m \frac{\partial^m}{\partial x^m} \left(\frac{x}{x^2+y^2} \right) \tag{56}$$

$$S_m(x,y) = \int_0^\infty k^m e^{-kx} \sin ky \, dk = (-1)^m \frac{\partial^m}{\partial x^m} \left(\frac{y}{x^2+y^2} \right), \quad m = 0, 1, 2, 3, \ldots \tag{57}$$

In Eq. (54) for different values of n, to obtain best approximation for $\frac{G}{\Delta}$, the least-square method is used by (Ben-Menahem and Gillon, 1970) and established that n = 2 yields satisfactory results for realistic earth models. So that, the approximation used is given by

$$\frac{G}{\Delta} \cong 1 + (A+Bk^2H^2)e^{-2Hk} + (C+\alpha' k^2 H^2)e^{-\beta' kH} \tag{58}$$

In Eqs. (38)-(42), using the approximation for $\frac{G}{\Delta}$ we have found that the expressions for stresses can be written as a linear combination of $S_m(x,y)$ and $C_m(x,y)$ for $m = 1, 2, 3, 4, 5$.

For numerical computations, the values of the parameters v, σ_1, σ_2, α', β' are taken from (Ben-Menahem and Gillon, 1970) for the continental earth model and are given in Table 1.

The following dimensionless quantities are defined for numerical computations.

$$Y = \frac{y}{h}, T = \frac{H}{h} \tag{59}$$

$$\Sigma_{23} = \frac{\pi h^2}{\mu_1 b ds} \tau_{23}^{(1)}, \Sigma_{33} = \frac{\pi h^2}{\mu_1 b ds} \tau_{33}^{(1)} \tag{60}$$

where h is the source depth

Discussion

We numerically study the variation of the normal and shear stresses with the epicentral distance due to horizontal and vertical tensile faults. We have used MATHEMATICA Wolfram (1991) software for symbolic and numerical computations.

Table 1: Parameters values

v	n	σ_1	σ_2	α'	β'
1.76	2	0.27	0.27	0.43871	3.31986
2.22	2	0.27	0.27	0.70360	3.22888
5.00	2	0.23	0.30	1.17574	2.92896

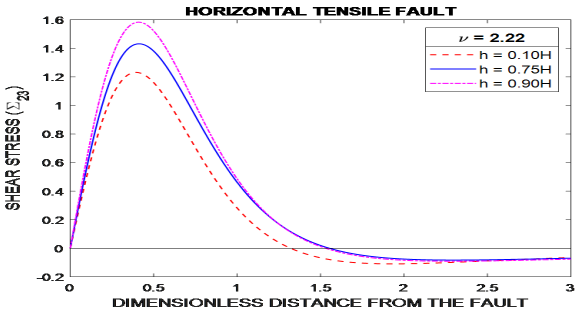

Figure 2: Variation of the dimensionless shear stress with the dimensionless distance from the fault due to a horizontal tensile fault for $\boldsymbol{\nu = 2.22}$ and h = 0.10H, 0.75H, 0.90H

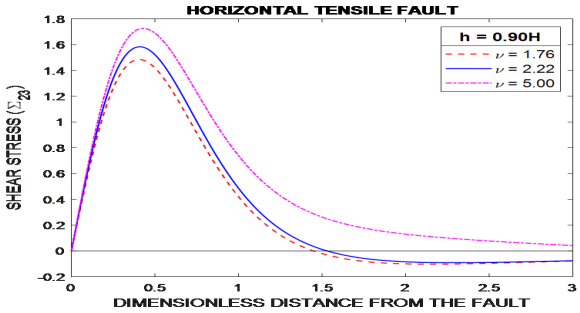

Figure 6: Variation of the dimensionless shear stress due to a horizontal tensile fault when the line source is situated at h = 0.90H and $\boldsymbol{\nu = 1.76, 2.22}$, 5.00

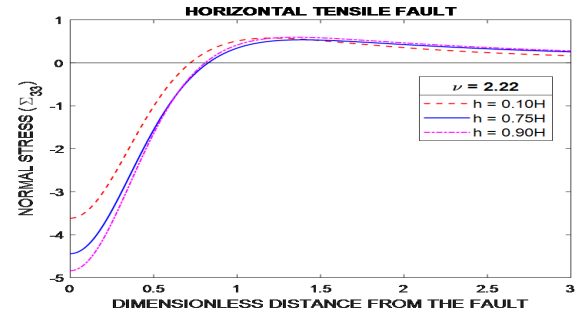

Figure 3: Variation of the dimensionless normal stress with the dimensionless distance from the fault due to a horizontal tensile fault for $\boldsymbol{\nu = 2.22}$ and h = 0.10H, 0.75H, 0.90H

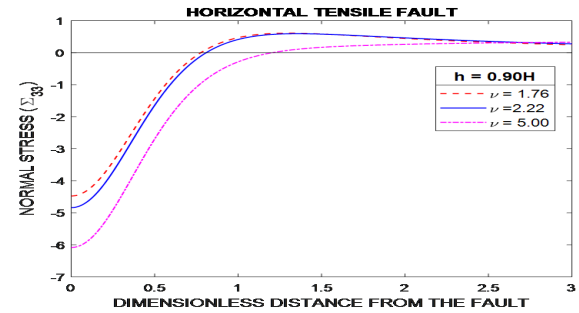

Figure 7: Variation of the dimensionless normal stress due to a horizontal tensile fault when the line source is situated at h = 0.90H and $\boldsymbol{\nu = 1.76, 2.22, 5.00}$

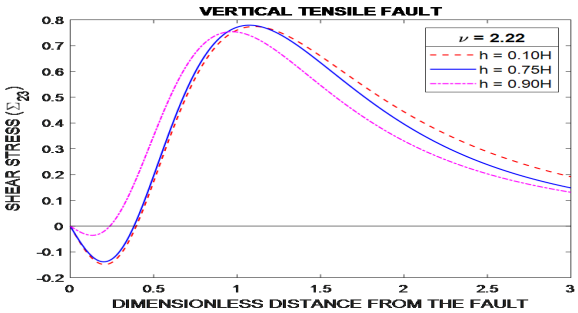

Figure 4: Variation of the dimensionless shear stress with the dimensionless distance from the fault due to a vertical tensile fault for $\boldsymbol{\nu = 2.22}$ and h = 0.10H, 0.75H, 0.90H

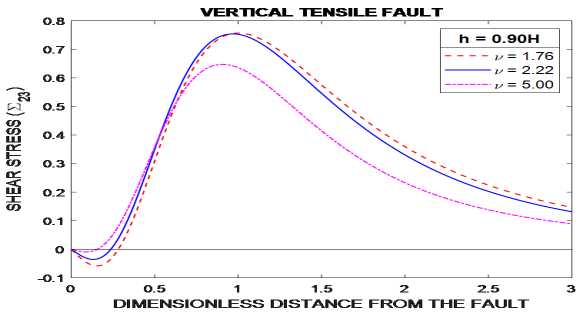

Figure 8: Variation of the dimensionless shear stress due to a vertical tensile fault when the line source is situated at h = 0.90H and $\nu = 1.76, 2.22, 5.00$

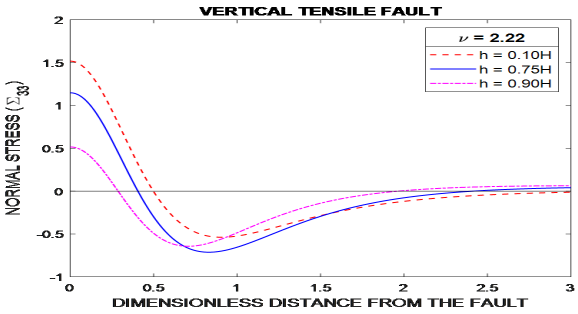

Figure 5: Variation of the dimensionless normal stress with the dimensionless distance from the fault due to a vertical tensile fault for $\boldsymbol{\nu = 2.22}$ and h = 0.10H, 0.75H, 0.90H

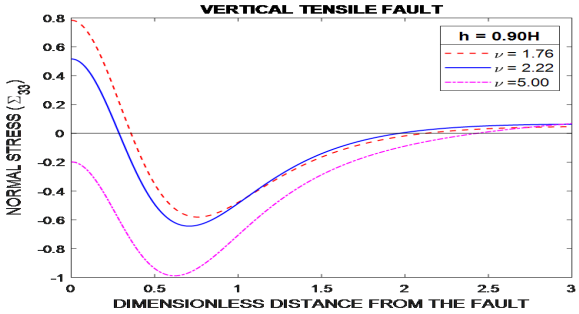

Figure 9: Variation of the dimensionless normal stress due to a vertical tensile fault when the line source is situated at h = 0.90H and $\nu = 1.76, 2.22, 5.00$

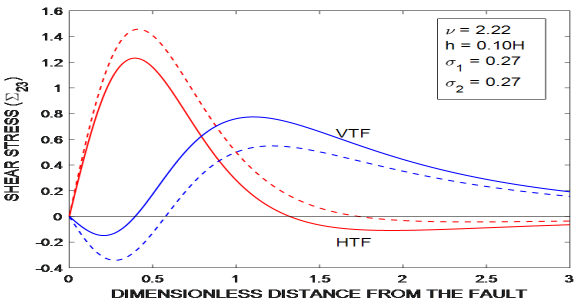

Figure 10: Variation of shear stress due to horizontal and vertical tensile fault for h = 0.10H and $\boldsymbol{\nu = 2.2}$

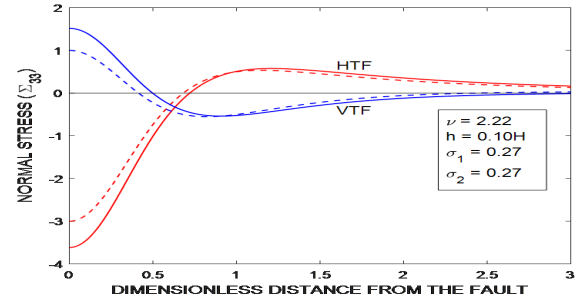

Figure 11: Variation of normal stress due to horizontal and vertical tensile fault for h = 0.10H and $\boldsymbol{\nu = 2.22}$

For three different values of the rigidity contrast, we have also studied the effect of source locations.

Figures 2 and 3 demonstrate the variation of the dimensionless shear $(\sum_{23})$ and normal $(\sum_{33})$ stresses, respectively, at the rigid surface of an elastic layer lying over an elastic half-space due to a horizontal tensile fault as the dimensionless distance changes for the rigidity ratio $v = \frac{\mu_2}{\mu_1} = 2.22$ (continental earth model) and $h = 0.10H, 0.75H, 0.90H$. The value of shear stress $(\sum_{23})$ in Figure 2 is $'0'$ at $Y = 0$ and its sign turns from positive to negative. Moreover, its value tends to zero as Y tends to infinity. We may observe that the magnitude of shear stress likewise increases with the source depth. As shown in Figure 3 the normal stress $(\sum_{33})$ changes from a negative to a positive value, and tends to zero as Y tends to infinity. It is also clear that the magnitude of normal stress increases initially with increasing source depth but then decreases as the source depth increases.

Figures 4 and 5 illustrate the variation of the dimensionless shear $(\sum_{23})$ and normal $(\sum_{33})$ stresses, respectively, at the surface due to a vertical tensile fault as the dimensionless distance changes for the rigidity ratio $v = \frac{\mu_2}{\mu_1} = 2.22$ (continental earth model) and $h = 0.10H, 0.75H, 0.90H$. Figure 4 shows that the shear stress $(\sum_{23})$ changes its sign from negative to positive and its value is $'0'$ at $Y = 0$. As the source depth increases magnitude of shear stress increases for some extent and after that its magnitude decreases with the source depth. For large value of fault depth $h = 0.90H$ stress field is much more influenced. From Figure 5, we can examine that as the fault depth increases, the magnitude of the normal stress initially decreases and subsequently increases. The magnitude of both stresses approaches $'0'$ as the distance from the fault approaches infinity.

The influence of the rigidity ratio on the shear stress $(\sum_{23})$ and normal stress $(\sum_{33})$ with the distance from the fault is exhibited in Figures 6 and 7, respectively, for the source depth $h = 0.90H$ due to a horizontal tensile fault. Figure 7 displays that for all values of v, shear stress vanishes at the origin. We investigate that as epicentral distance increases magnitude of shear stress and normal stress increases with the increase in the value of v. For large value $h = 0.90H$ of source depth the effect of rigidity is more influential for $v = 5.00$. But for all values of v, as epicentral distance approaches to infinity magnitude of both components of stress approaches to zero.

Figures 8 and 9 depict variation of the shear $(\sum_{23})$ and normal $(\sum_{33})$ stresses, respectively, with the dimensionless horizontal distance due to a vertical tensile fault for $h = 0.90H$ and display the effect of the rigidity ratio on the stress field. We can analyse that the rigidity ratio has more influence in case of normal stress while its effect is less experienced in case of shear stress. The shear stress $\sum_{23} = 0$ for $Y = 0$ and both the stresses tends to $'0'$ as $Y \to \infty$. Figure 9 investigates that the value of the normal stress $(\sum_{33})$ decreases as the rigidity ratio (v) increases.

Figure 10 represents the variation in shear stress $(\sum_{23})$ with the distance due to a horizontal and vertical tensile fault for $v = 2.22$ and $h = 0.10H$. For layered half-space, the variation of the shear stress is shown by continuous lines, on the other hand dashed lines depict the variation in the stress field for a uniform half-space. The shear stress $(\sum_{23})$ changes its sign from positive to negative for both uniform and layered half-spaces in case of horizontal tensile fault, while its sign changes from negative to positive in case of vertical tensile fault for both uniform and layered elastic half-spaces. It can also be seen that effect of the underlying medium is significant near the interface while near the rigid surface, its effect is insignificant.

The effect of underlying half-space is observed in Figure 11 on the normal stress $(\sum_{33})$ with the distance from the fault due to a horizontal and vertical tensile fault for $v = 2.22$ and $h = 0.10H$. For layered half-space, continuous lines reflect the variation of the normal stress, whereas dashed lines show variation of stress field for uniform half-space. In case of layered half, near the origin normal stress $(\sum_{33})$ is positive in case of vertical tensile fault, while its value is more negative in case of horizontal tensile fault. In all cases normal stress $(\sum_{33})$ approaches to $'0'$ as the distance from the fault approaches to $'\infty'$.

Conclusion

The 2-D plane strain static solution for multi-layered half-space composed of a rigid boundary elastic layer in welded contact with an elastic half-space has been obtained in this investigation.

In the case of a horizontal tensile fault, the magnitude of shear stress and normal stress increases with the increasing value of the source depth.

As the rigidity ratio increases, the magnitude of shear and normal stresses increases for the horizontal tensile fault.

In the case of a vertical tensile fault, the normal stress is significantly more influenced by the source depth and rigidity ratio, and its magnitude diminishes as the source depth and rigidity ratio increase.

Acknowledgment

All authors thank the reviewers for their helpful remarks that improved the work.

References

Ben-Menahem, A., & Gillon, A. (1970). Crustal deformation by earthquakes and explosions. *Bulletin of the Seismological Society of America*, 60, 193-215.

Ben-Menahem, A., & Singh, S. J. (1968). Multipolar elastic fields in a layered half. *Bulletin of the Seismological Society of America,* 58, 1519-1572.

Chugh, S., Madan, D. K., & Singh, K. (2011). Static deformation of an orthotropic elastic layered medium due to a non-uniform discontinuity along a very long strike-slip fault. *International Journal of Engineering, Science and Technology*, 3(1), 69-86.

Gradshteyn, I. S., Ryzhik, I. M., & Romer, R. H. (1988). Tables of integrals: Series and products. *American Journal of Physics*, 56, 958-958.

Kumari, A., & Madan, D. K. (2022). Stresses caused by vertical dip-slip fault embedded in an isotropic half-space joined perfectly with an orthotropic half-space. *International Conference on Advances in Multi-Disciplinary Sciences and Engineering Research, AIP Conference Proceedings,* 020079-1-020079-11.

Kundu, P., & Sarkar(Mondal), S. (2021). Deformation of an elastic layer overlying an elastic half-space caused by a finite, buried, inclined, locked strike-slip fault. *Recent Trends in Applied Mathematics, Lecture Notes in Mechanical Engineering*, 283-306.

Kundu, P., Sarkar(Mondal), S., & Mondal, D. (2021). Creeping effect across a buried, inclined, finite strike-slip fault in an elastic layer overlying an elastic half-space. *GEM- International Journal on Geomathematics*, 2021(12:2), 1-33.

Madan, D. K., & Gaba, A. (2016). 2-Dimensional deformation of an irregular orthotropic elastic medium. *IOSR Journal of Mathematics*, 12(4), 101-113.

Madan, D. K., & Kumari, A. (2022). Stresses and displacements for two imperfectly joined half-spaces induced by vertical tensile fault. *Proceedings of the Indian National Science Academy*, 88, 104-115.

Manna, K., & Sen, S. (2017). Interacting inclined strike-slip faults in a layered medium. *Mausam Quarterly Journal of Meteorology, Hydrology and Geophysics*, 68(3), 487-498.

Maruyama, T. (1964). Statical elastic dislocations in an infinite and semi-infinite medium. *Bulletin of the Earthquake Research Institute*, 42, 289-368.

Maruyama, T. (1966). On two-dimensional elastic dislocations in an infinite and semi-infinite medium. *Bulletin of the Earthquake Research Institute*, 44, 811-871.

Pakhare, K. S., Sawhney, H., Shimpi, R. P., Guruprasad, P. J., & Desai, Y. M. (2021). Analytical and numerical investigations of the flexure of isotropic plates using the novel first-order shear deformation theory. *Proceedings of the Indian National Science Academy*, 87, 379-392.

Rani, D., & Rani, S. (2024). Deformation of a layered elastic medium due to an inclined long strike-slip fault. *Journal of Earth System Science*, 133(69), 1-14.

Rani, S., & Singh, S. J. (1992). Static deformation of a uniform half-space due to a long dip-slip fault. *Geophysical Journal International*, 109, 469-476.

Rani, S., & Singh, S. J. (2007). Quasi-static deformation due to two-dimensional seismic sources embedded in an elastic half-space in welded contact with a poroelastic half-space. *Journal of Earth System Science*, 116, 99-111.

Rani, S., Singh, S. J., & Garg, N. R. (1991). Displacement and stresses at any point of a uniform half-space due to two-dimensional buried sources. *Physics of the Earth Planetary Interiors*, 65, 276-282.

Sangeeta., Malik, M., & Sikka, S. J. (2023). Static deformation caused by a tensile fault embedded in an isotropic half-space perfectly joined with an orthotropic half-space. *European Chemical Bulletin*, 12(7), 8600-8611.

Savage, J. C. (1998). Displacement field for an edge dislocation in a layered half-space. *Journal of Geophysical Research Solid Earth*. 103, 2439-2446.

Savita., Sahrawat, R. K., & Malik, M. (2022). Tensile fault dislocation in an irregular-layered elastic half-space. *International Journal of Applied Mechanics and Engineering*, 27(3), 171-198.

Singh, M., & Singh, S. J. (2000). Deformation of a uniform half-space due to a very long tensile fault. *ISET Journal of Earthquake Technology*, 37, 27-38.

Singh, S. J., & Garg, N. R. (1986). On the representation of two-dimensional seismic sources. *Acta Geophysica Polonica*, 34, 1-12.

Singh, S. J., & Rani, S. (1991). Static deformation due to two-dimensional seismic sources embedded in an isotropic half-space in welded contact with an orthotropic half-space. *Journal of Physics of the Earth*, 39, 599-618.

Singh, S. J., & Singh, M. (2004). Deformation of a layered half-space due to a very long tensile fault. *Proceedings of the Indian Academy Sciences-Earth and Planetary Sciences*, 113, 235-246.

Singh, S. J., Punia, M., & Kumari, G. (1997). Deformation of a layered half-space due to a very dip-slip fault. *Proceedings of the Indian National Science Academy*, 63, 225-240.

Sneddon, I. N. (1951). Fourier Transforms. *McGraw-Hill*, New York.

Sokolnikoff, I. S., & Specht, R. D. (1956). Mathematical Theory of Elasticity. *McGraw-Hill*, New York.

Soni, N., & Rani, S. (2023). Lithospheric plane strain deformation caused by a vertical dip-slip fault. *Journal of Earth System Science*, 132(178), 1-28.

Steketee, J. A. (1958a). On Volterra's dislocations in a semi-infinite elastic medium. *Canadian Journal of Physics*, 36, 192-205.

Steketee, J. A. (1958b). Geophysical applications of the elasticity theory of dislocations. *Canadian Journal of Physics*, 36: 1168-1198.

Wolfram, S. (1991). Mathematica: A System for Doing Mathematics by Computer. *Addison Wesley*, California.